

Current reversal in polar flock at order-disorder interface

Jay Prakash Singh^{1,2,*} Partha Sarathi Mondal^{1,†} Vivek Semwal^{1,‡} and Shradha Mishra^{1,§}

¹ *Indian Institute of Technology (BHU) Varanasi, India 221005*

² *Israel Institute of Technology, Technion Haifa Israel*

(Dated: February 16, 2023)

We studied a system of polar self-propelled particles (SPPs) on a thin rectangular channel designed into three regions of order-disorder. The division of the three regions is made on the basis of the noise SPPs experience in the respective regions. The noise in the two wide region is chosen lower than the critical noise of order-disorder transition and noise in the middle region or interface is higher than the critical noise. This make the geometry of the system analogous to the Josephson Junction (JJ) in solid state physics. Keeping all other parameters fixed, we study the properties of the moving SPPs in the bulk as well as along the interface for different widths of the junction. On increasing interface width, system shows a order-to-disorder transition from coherent moving SPPs in the whole system to the interrupted current for large interface width. Surprisingly, inside the interface we observed the current reversal for intermediate widths of the interface. Such current reversal is due to the strong randomness present inside the interface, that makes the wall of the interface reflecting. Hence Our study give a new interesting collective properties of SPPs at the interface which can be useful to design devices like switch using active agents.

I. INTRODUCTION

Emergence of collective motion [1–5] and global ordering [6–11] among the various living or non-living systems, are well known phenomena. Each particle show systematic motion at the cost of its internal energy. All individuals in a group synchronize themselves to show different behavioral state, exhibiting host of interesting properties like pattern formation [12], non equilibrium phase transition [7], large density fluctuation [12–16], enhance dynamics [17–26], motility induced phase separation [27–31] etc.,. Interestingly, different real biological systems are encountered with different kinds of confined geometry [32–37]. Confinement and boundary play significant role in variety of biological systems [33], sheared systems [38], other places like in fluid dynamics. Boundary can induce many interesting phenomena like, spontaneous flow inside the channel [39], and another classic example include Rayleigh-Benard convection in the fluid [40]. There are variety of practical applications based on confined geometry like; mass transport in nanofluids to enhance the microfluidic devices [41, 42], geophysical applications etc.,.

There are few studies where researchers have seen the behaviour of SPPs at the interface of two different substrate media. Most of studies involves the media of two dissimilar fluids [43–46]. For example, Dirichlet et al. [47] observed that catalytic active Brownian microswimmer at different solid-liquid interface shows inhomogeneity in the particles speeds with respect to the orientation of catalytic substrate at different interface. Another well known classical example of interface between supercon-

ductor and insulator with boundary is Josephson Junction (JJ) in solid state system [48–52].

Motivated with the JJ in solid state, here in this article we will discuss the collective properties of SPPs by designing a setup analogous to JJ. We have modeled a system of polar SPPs with alignment interaction through a thin rectangular narrow channel. Further, the thin channel is divided into three regions wherein two opposite regions, SPPs move coherently. In the middle region SPPs diffuse randomly and no net current. Although the comparison between our setup and Josephson junction is not very common, since the superconducting phenomena are macroscopically quantum in nature, but we still designed an analogous model system for collection of SPPs and observe the properties of it.

We also studied the case where a small external field is introduced, along the long axis of the system which gives an easy direction for particle alignment. System is studied for different widths of the intermediate disorder region with and without easy direction (perturbation). On tuning the width of the disorder region, SPPs with perturbation shows a non-equilibrium phase transition whereas without perturbation, it shows a weak dependence on the interface width. Further, at the junction, particles get reflected from it's walls and we observed the current reversal. This lead to the some of the SPPs to move in opposite direction and hence contribute in negative current. We also showed one application of the system geometry to use it for sorting two different type of SPPs.

Rest of the manuscript is divided as follows; we have discussed the details of the model in section II. The results are discussed in section III, one possible application in section IV and conclusion of the paper with summary is discussed in section V.

* jayps.rs.phy16@itbhu.ac.in

† parthasarathimondal.rs.phy21@itbhu.ac.in

‡ viveksemwal.rs.phy17@itbhu.ac.in

§ smishra.phy@itbhu.ac.in

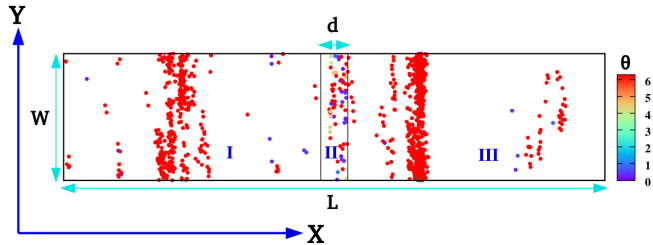


FIG. 1: (color online) We show a model picture of the system obtained from the simulation in which different color shows particle's orientation $\theta \in [0, 2\pi)$. The region II is the interface (junction) with disorder region whereas the region to the left and right of the interface (I & III) is the ordered region. Noise strength in region II is $\eta_{II} = 0.7$ and in regions I, III $\eta_I = \eta_{III} = 0.3$. d is the width of the interface. The two vertical lines in the middle indicate the boundary of the interface. The W and L are the short and long dimensions of the system. The axis for the two directions of the system is drawn on the left. Periodic boundary condition is used in both the directions.

II. MODEL

We consider a collection of polar self-propelled particles (SPPs) moving on a two-dimensional substrate on a rectangular narrow channel with periodic boundary conditions (PBC) in both directions. The short and long axis of the channel are denoted by W and L , respectively as shown in fig.1. Particles interact through a short-range alignment interaction within a small interaction radius $R_0 = 1$ [7]. Moreover, the strength of interaction of each SPP is the same. The system is partitioned into three regions: the two regions on the left and right represent the ordered region and third middle section shows the disordered region. The middle disordered region is termed as junction or interface and the width d of the interface is our tuning parameter. The width of the junction is varied from $d = (1 - 30)$. In three regions, each particle is defined by its position $\mathbf{r}_i(t)$ and orientation $\theta_i(t)$ at time t and they move along the direction of their orientation with a fixed speed $v_0 = 0.5$. The position and orientation updates of a particle are given by:

$$\mathbf{r}_i(t + \Delta t) = \mathbf{r}_i(t) + v_0 \mathbf{n}_i \Delta t \quad (1)$$

$$\mathbf{n}_i(t + \Delta t) = \frac{\sum_{j \in R_0} \mathbf{n}_j(t) + \eta_{i,k} N_i(t) \xi_i(t)}{w_i(t)} \quad (2)$$

where, $\Delta t = 1.0$ is the unit-time step and $\mathbf{n}_i = (\cos \theta_i, \sin \theta_i)$ is the unit direction vector of the i^{th} particle. In eq.2, the first term in the right hand side represents the short-range alignment interaction inside the interaction radius (R_0) of the i^{th} particle. The second term $\xi_i(t) = (\cos(\phi_i(t)), \sin(\phi_i(t)))$ on the right hand side of eq.2 denotes the vector noise which measures the error made by the particle, following its neighbors. ϕ_i is

uniform random angle $\in (-\pi, \pi)$, $N_i(t)$ denote the number of neighbors within the interaction radius of the i^{th} particle at time t . Further, $\eta_{i,k}$ ($k = I, II$ and III) ($\eta_I = \eta_{III} = 0.3$ and $\eta_{II} = 0.7$) shows the strength of the randomness present in the system for the three regions. We choose the mentioned values of noise, because for the clean polar SPPs interacting through Vicsek type alignment interaction with vector noise, the order-disorder transition occurs at $\eta \sim 0.6$ (for the same set of parameters used here)[53, 54]. $w_i(t)$ is the normalisation factor which reduces the right hand side of the eq.2 to a unit vector. The above model we called as system without perturbation (WOP).

Due to the rectangular geometry of the system, particle experiences an easy axis for their motion (along the long axis of the system). We also introduced an external perturbation along the long-axis of the channel. It gives an easy direction for the SPPs motion; hence the orientation update equation will become

$$\mathbf{n}_i(t + \Delta t) = \frac{\sum_{j \in R_0} \mathbf{n}_j(t) + h_0 \mathbf{n}_p + \eta_k N_i(t) \xi_i(t)}{w_i(t)} \quad (3)$$

here, h_0 is the strength of the external field and kept fixed to a small value with direction $\mathbf{n}_p = (1, 0)$. Using the above equation eq.3, the model is referred to as system with perturbation (WP). Further, number density of SPPs is defined by $\rho = \frac{N}{L \times W} = 1.0$, where N is the total number of particles in the system. All the particles are allowed to move throughout the system and they experience the noise of different regions accordingly. We let the system evolve from random homogeneous state of density and orientation of particles. All the results discussed below are in the steady state, and total time step of the simulation is taken 10^6 . One simulation step is counted after the update of all the particles once. Numerical details and parameters are as chosen as $R_0 = 1.0$, $L = 200, 400$, $W = 5$, and h_0 is varied from 2% to 6% of the strength of alignment; which is fixed to 1. A total 20 independent realisations are used for better statistics.

III. RESULTS

A. Global ordering and junction width (d)

First, we study the effect of junction width d on the global orientation in the whole system of size $L \times W = 200 \times 5$ for different junction widths d . Ordering in the system is characterized by the orientation order parameter,

$$\Psi(t) = \frac{1}{N} \left| \sum_{i=1}^N n_i(t) \right| \quad (4)$$

In the ordered state, i.e., when majority of particles are moving in the same direction, then Ψ will be closer to 1, and of the order of $\frac{1}{\sqrt{N}}$ for a random disordered state. First, we show the variation of $\Psi = \langle \Psi(t) \rangle$, where,

$\langle \dots \rangle$ means average over time in the steady state and over 20 independent realisations. We first study the system WOP. In fig.2(a), we plot Ψ vs. junction width d and found that with increase in d , Ψ shows small decay, which have been further confirmed by orientation probability distribution function (PDF) $P(\Psi)$ in fig2(b). To understand the small decay of Ψ with width d , we have shown the snapshots for two different junction widths $d = 2$ and 18 in fig.2(b) and (c), respectively. The circles represent the particle and color of the circle shows their orientations. In general the SPPs form the ordered band inside the ordered region as shown by the dense moving SPPs along the channel in fig.2(b) (from right direction). The size of the ordered band or cluster depends on the chosen set of system parameters [14, 55, 56]. Hence for small width as shown in fig.2(b), when the width of the interface is smaller or of the order of the size of the band, the SPP passes the interface before it experiences the disorder present inside the interface. Hence the global order parameter retains high value ~ 0.8 and direction of moving SPPs band remains unaffected after interaction with the interface (shown by the almost a clear common orientation of all particles in the system in fig.2(b)). As we increase the width of the interface, and the width of the disordered region is larger than the size of the band. Then before the band can pass the interface it experiences the disturbance and front of the band randomise. Due to that the particles moving at the back also feel random orientation before they enter the interface. Hence, a part of the band reorient before it can pass the interface as shown in fig.3(a-b). The whole process looks like a reflection due to the interface as in fig.3(c-d). Some part of the band able to come out of the interface from the other side and they contribute the forward moving current, but a finite fraction of particles from the band observe reflection from the walls of the interface as shown in fig.3(e-f). A clear animation of the interaction of a band with the interface is shown in SM1. The interface acts like a partially reflecting wall, it leads the SPPs to avoid the junction. Also to avoid the interface their orientation develops some contribution in Y -direction as well. As shown in the snapshots fig.3(e-f), the orientation of particles are not strictly along $\theta = (0, \pi \text{ or } 2\pi)$. This reduces their frequency of going inside the interface. This results that mostly the SPPs are moving in the ordered region only, and we find weak dependence of global order parameter on the width d .

Further, we have studied the system WP. The perturbation introduced in such a way that flock is biased to move along the $+ve$ direction of long axis (x -axis). Interestingly, we have found that global orientation order parameter Ψ decay sharply with an increase in the junction width d as shown in fig.4(a). Which has been confirmed by plotting the probability distribution function (PDF) $P(\Psi)$ for different junction widths d in inset of fig.4(a).

Fig.4(b)-(c) show the plot the snapshots for different junction widths $d = 2$ and 18. For lower width of junction flock does not experience any hurdle and passes coherently with different bands, leads to higher values of

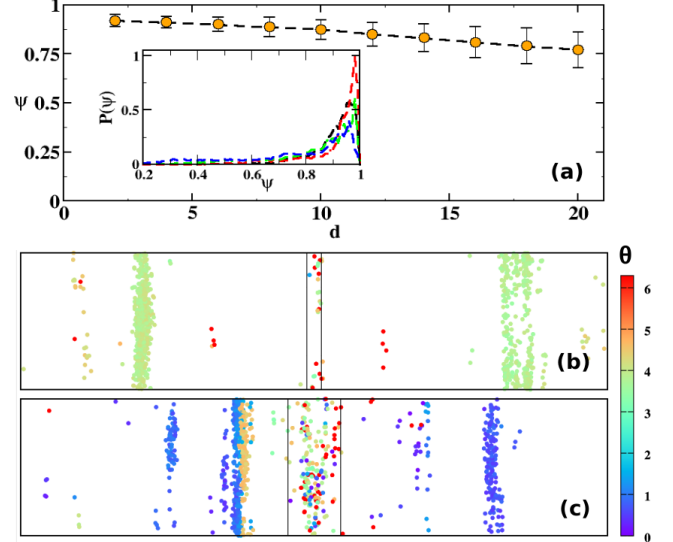


FIG. 2: (color online) All the plots (a)-(c) shown here for without perturbation. (a) We plot the global orientation order parameter Ψ vs. width of the disorder region d . Inset;(a) plot shows the global order parameter distribution $P(\Psi)$ for different width of the junction d . Different colored break lines are for $d = 4$ (black), $d = 8$ (red), $d = 12$ (green) and $d = 18$ (blue). Plot (b) and (c) show the space snapshots of the system for width $d = 5$ and $d = 18$ respectively. color of each particle represents it's orientation $\theta \in [0, 2\pi]$ according to the color bar. $L \times W = 200 \times 5$ and $\rho = 1.0$

Ψ . Moreover, for higher values of junction width, most of the SPPs trapped into the junction with random directions hence decreases in the value of Ψ . This is very different from what we observed for system WOP as shown in fig.2(c) and fig.3, where the boundary of the interface acts like reflecting walls. But for the system WP, due to an easy direction for the moving band of SPPs, they are forced to enter inside the interface. Inside the interface the strength of the external perturbation is not strong enough to help them to pass. But it oppose their orientation in other direction. Hence particles feel a kind of frustration inside and spend more time in the junction as shown in the fig.4(c) and leads to small order parameter for large junction width d . In fig.5(a-f) we show the interaction of a band moving towards the interface at different times. We found that a moving band experiences some fluctuation from the interface, but density inside the junction is large as shown in fig.5(c-d), and finally the particles get out of the junction from the other side without getting a clear reflection as found for the case WOP (as shown in fig.5(e-f)). The details of interaction of a band with interface for system WP is shown in SM2. Further we study the properties of the flock along the interface in system without perturbation.

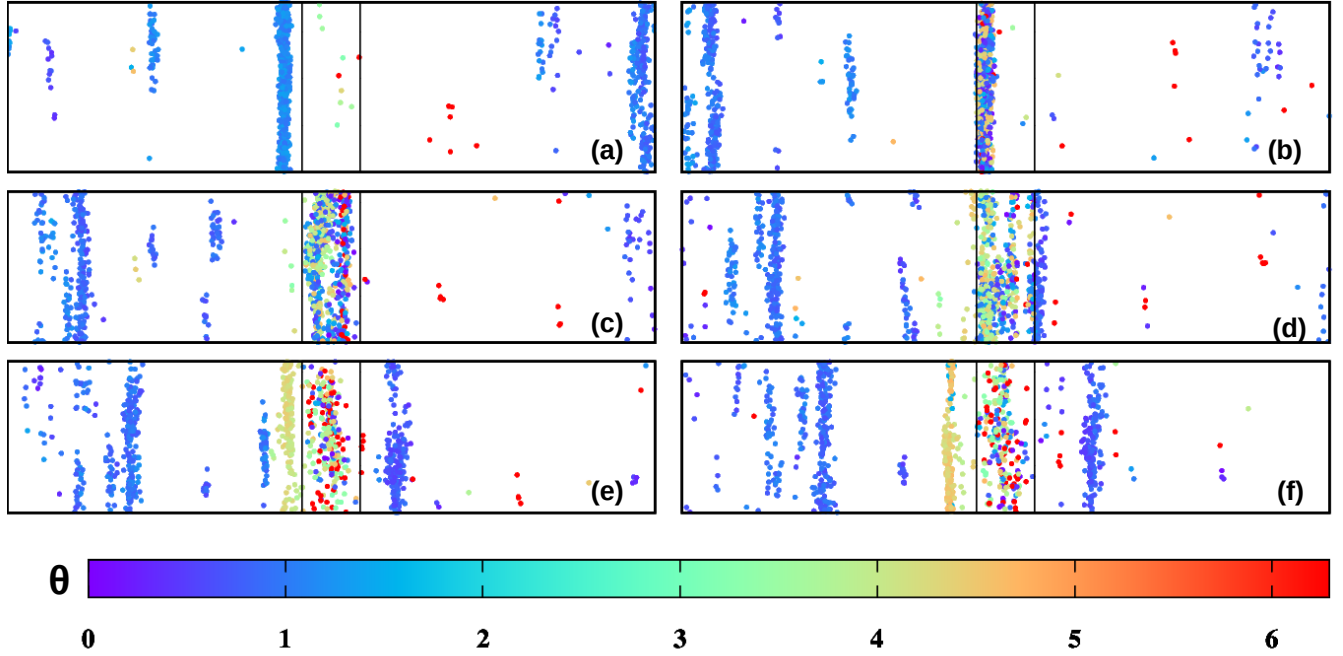


FIG. 3: (color online) Snapshots of particles (for system WOP) with their orientation angle θ shown in color bar at times $t = 2122, 2163, 2204, 2223, 2253$ and 2271 (a-f) respectively. The time is chosen such that a dense band of particles moving towards the interface (blue color) in (a), enter inside the junction (b) and a part of the particles inside the band start getting reflected (having orientation towards $-x$ direction) (c-d) and macroscopic fraction of particles are reflected from the interface as shown in (e-f). Some part of particles are transmitted through the junction (e-f). The width of the interface $d = 14$, $L \times W = 200 \times 5$ and $\rho = 1.0$

B. Current inside the junction

Junction current:- In this section, we discuss the junction current within the junction along the long x -axis as well as y -axis with the variation of the junction width d . The junction current is calculated when at least 25% particles of the whole system are within the junction, and we named this current as event current. The event current in the junction along x and y -directions is defined by $\Psi_{xd}(t) = \frac{1}{n} \sum_i^n v_{xi}$, $\Psi_{yd} = \frac{1}{n} \sum_i^n v_{yi}$ and finally total event current $\Psi_d(t) = \frac{1}{n} |\sum_i^n n_i(t)|$. where v_{xi}, v_{yi} , and n represent the components of velocity vector along the long and short axis, and the total number of particles within the junction respectively. In the fig.6(a)-(c) We show the time series of Ψ_{xd} for different values of junction width d . We observe, with increased d , the amplitude of Ψ_{xd} decreases and also positive and negative current changes in a periodic fashion with the decreased period. Here current is carried by the particles along $+ve$ and $-ve$ x -direction, we call them positive and negative currents respectively. Further, in fig.6(d); we show the current probability distribution function $P(\Psi_{xd})$ of Ψ_{xd} . It clearly suggests that with the increase in the width of the junction, there is a clear signature of current reversal. Also, in fig.6(e) we plot the current-current auto-

correlation function $C(\Psi_{xd}) = \langle \Psi_{xd} \cdot \Psi_{xd} \rangle$. Sharper decay of auto-correlation with the increase in the junction width d . Hence we find that in the channel the current along the long axis alternate from $+ve$ to $-ve$ on tuning the width d . Here our claim regarding current reversal phenomena is very interesting properties of the flock at the junction. For small widths $d < 8$, coherent flock enters into the junction and crosses without significant deviation. For intermediate widths $8 \leq d \leq 16$, we observed that once coherent moving SPPs enters into the junction, it faces a randomness inside the junction. Since inside the junction all the directions are equally probable, but flock prefers to move in $+ve$ or $-ve$; x -direction, that lead to the quicker escape from the disorder region. Further SPPs try to come out from the junction and stabilizes back and forth oscillations within the junction. This oscillation along $+ve$ and $-ve$ x -direction, we are calling alternating change in the orientation event current. Interestingly this oscillation is more prominent for the intermediate junction widths $8 \leq d \leq 16$. For small width of the junction the extend of the moving bands of SPPs is of the order or larger than the width of the interface and SPPs can easily pass through it with small disturbance hence the x -current Ψ_{xd} shows small oscillations with time and no negative current. But as we increase the width of the interface, when the size

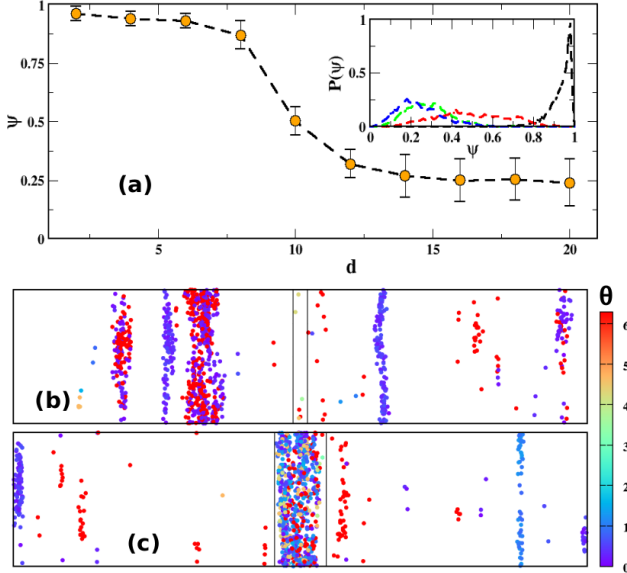


FIG. 4: (color online) All the plots (a)-(c) shown here for with perturbation. (a) We plot the global orientation order parameter Ψ vs. width of the disorder region d with perturbation. Inset;(a) plot shows the global order parameter distribution $P(\Psi)$ for different width of the junction d . Different colored break lines are for $d = 4$ (black), $d = 8$ (red), $d = 12$ (green) and $d = 18$ (blue). color of each particle represents its orientation $\theta \in [0, 2\pi]$ according to the color bar. Plot (b) and (c) show the space snapshots of the system for width $d = 5$ and $d = 18$ respectively. The two vertical lines indicate the boundary of the interface. $L \times W = 200 \times 5$ and $\rho = 1.0$

of the interface is larger than the size of the ordered band, then for some distance the moving band of SPPs is able to penetrate (which is analogous to the penetration depth in solid state) and then experience randomness. Which leads to a fraction of particles from the moving band reverses its direction of motion and we experience a negative current and hence negative Ψ_{xd} as shown in fig.6(b-c). This leads to the phenomena of current reversal inside the junction. For widths $d > 20$, moving SPPs experience more and more reflection and unable to enter inside the junction and gets reflected from the wall itself and hence we have weak junction current. Due to that the magnitude of the junction current Ψ_{xd} decreases with increasing d . Furthermore, in fig.7(a)-(c), we show the junction current Ψ_{yd} and current PDF $P(\Psi_{yd})$ along the small axis with respect to junction width d . We observe that there is no current reversal with the increase in d . However, for higher d , there is a periodicity which is further confirmed by the current distribution $P(\Psi_{yd})$ is shown shown in fig.7(d).

C. Fraction of particles inside the junction

Till now, we have discussed about the orientation of moving SPPs inside the junction. We also find interesting results for the fraction of particles inside the junction $f(t) = \frac{\mathcal{N}(t)}{N}$. Here $\mathcal{N}(t)$ is the number of particles inside the junction at time t . We compared the probability distribution function (PDF) of $f(t)$ for the systems WOP and WP. The PDF, $P(f)$ is obtained by calculating the normalised distribution of fraction of particles inside the junction and then PDF is averaged different independent realisations.

In fig.8(a-d) we show the plot of $P(f)$ vs. f for different junction widths ($d = 4 - 20$) for the WOP and WP for three different strengths of perturbations 2%, 4% and 6% respectively. For all the cases the tail of the distribution extends on increasing width of the interface d , due to the increased area of the interface and hence more number of particles inside the junction. For all junction widths the PDF is power law with slope $f^{-1.25}$ for system WOP (as shown by log-log plot in the main plot of fig.8(a)). It suggests probability of finding all possible fractions of particles for system WOP. The inset fig.8(a) shows the same plot on log-y scale, to compare that the distribution is clearly power law, and not an exponential. For the system WP, the distribution clearly has deviation from power law and shows a clear peak for f close to 1 as shown in fig.8(b-d). The height of peak increases on increasing width d . For larger width and small perturbation 2% (fig.8(b)) a macroscopic fraction of particles spend time inside the junction. The appearance of peak close to $f \simeq 1$ is visible more clearly in the inset plot of fig.8(b), which is shown on log-y scale. As we increase the perturbation further the peak at larger f starts to weaken and distribution get flattens for intermediate f 's. It starts to appear more exponential in nature for larger perturbations $\geq 4\%$ as shown in the insets of fig.8(c-d), which are drawn on log-y scale. The exponential nature of the tail of the distribution represents a critical fraction of particles inside the junction. For 6% perturbation (fig.8(d) (main figure)), the distribution shows a power law decay with power f^{-1} for moderate f 's. It suggests the moderate fraction of particles inside the junction.

Here we summarise the behaviour of density of particles inside the junction. Adding a finite perturbation ease the SPPs to get in the interface. For weak perturbation although perturbation is enough for SPPs to enter the junction, but not sufficient for them to overcome the randomness present there. This lead to accumulation of particles inside the junction for some time. Hence a macroscopic fraction of particles spend time inside the junction and $P(f)$ shows a peak at $f \simeq 1$. As we increase the perturbation it lead to quicker entry of SPPs to the junction but now perturbation is comparable to the randomness present inside and they experience frustration inside the junction. This is visible by flattened power law feature of $P(f) \simeq f^{-1}$ for higher perturbations.

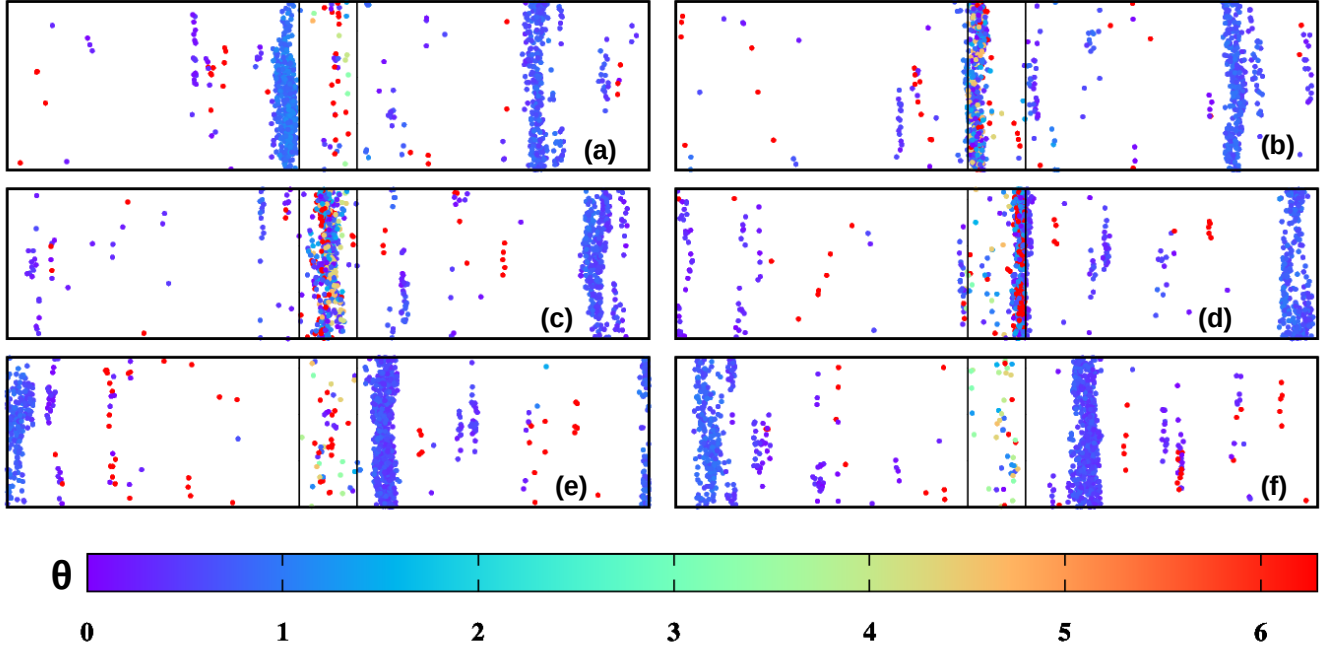


FIG. 5: (color online) Snapshots of particles with their orientation θ (shown in colorbar) inside the junction at times $t = 2101, 2125, 2150, 2175, 2195$ and 2220 from (a-f) respectively for system WP ($h_0 = 6\%$). There is no clear reflection of the particles from the interface. Other details of the system is the same as in fig.3.

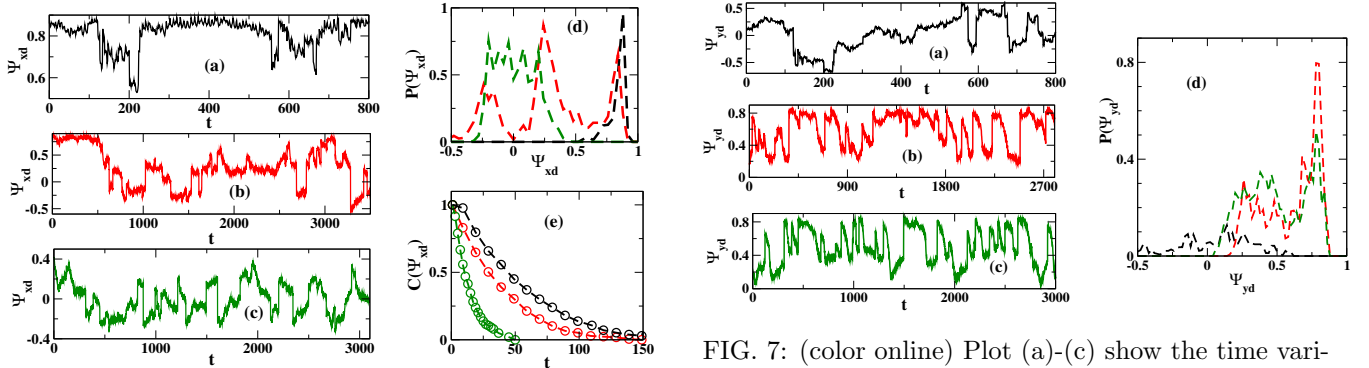


FIG. 6: (color online) Plot (a)-(c) show the time variation of event current Ψ_{xd} along the long axis with increasing width d . (d) event current distribution $P(\Psi_{xd})$. (e) Shows the x-orientation current auto correlation for three junction width d . Black, red and green colors show the results for junction width $d = 4, 8$ and 12 respectively. $L \times W = 200 \times 5$ and $\rho = 1.0$.

Till now, we have discussed the results for the same type of SPPs in the system. In the next section IV we show a one good application of such geometry, where junction can be used for sorting of particles.

FIG. 7: (color online) Plot (a)-(c) show the time variation of orientation event current Ψ_{yd} along the short axis with increasing width d . (d) Orientation event current distribution $P(\Psi_{yd})$. Black, red and green colors show the junction width $d = 4, 8$ and 12 respectively. $L \times W = 200 \times 5$ and $\rho = 1.0$.

IV. JUNCTION AS A PARTICLE SORTER

In this section we propose that such geometry of system for the case WOP: can also be used for the sorting two type of particles. As described earlier, for low and intermediate junction widths the particles travel in bands even after passing through the junction. Because of the periodic boundary condition, with time the band passes through the junction multiple times and after some time the particles separate into multiple narrow bands which

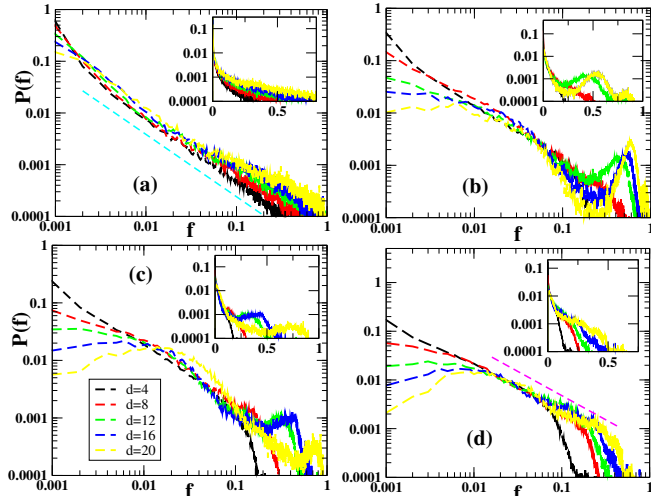


FIG. 8: (color online) Probability distribution, $P(f)$, inside the junction: Plot (a) is for WOP case and plots (b),(c),(d) are for WP case with perturbation strength (h_0) 2%, 4% and 6% respectively on log log scale. Colors 'black', 'red', 'green', 'blue' and 'yellow' corresponds to $d = 4, 8, 12, 16$ and 20 respectively. Insets shows the plot of $P(f)$ vs f in log $-y$ scale. In plot (a) the dashed line (cyan) is the power law with exponent 1.25 and in plot (d) dashed line (magenta) is power law with exponent 1. $L \times W = 200 \times 5$ and $\rho = 1.0$.

have some dynamics in the transverse direction as well. This motivated us to think: what will happen if we place a mixture of two different types of particles in the system?

To investigate that we considered a mixture of two different type of particles (1 & 2) distributed with random orientation and position in the system.

Two type of particles differ in their response to the noise: angle of the random vector noise $\phi \in (-0.9\pi, +1.1\pi)$ for one type and $\phi \in (-1.1\pi, +0.9\pi)$ for the other. Hence one type particles have noise with mean 0.1π and the noise has mean -0.1π for the second types. Hence through noise, we have introduced a random clockwise and anticlockwise chirality for the two type of particles. Also the strength of alignment interaction is much stronger for particles of its own type compared to the other type (1.0 and 0.5 respectively). Results showed that after some time two different types of particles form separate bands (data not shown). To characterize this, we define the phase separation order parameter for both types ($P_{1,2}$) as:

$$P_k = \frac{1}{N_k} \sum_{i=1}^{N_k} \left| \frac{N_s(i) - N_d(i)}{N_s(i) + N_d(i)} \right| \quad (5)$$

where, $k = 1, 2$ is the index used to denote two different types with N_1, N_2 being total number of particles of respective types. For k^{th} type, $N_s(i), N_d(i)$ respectively denote number of particles of similar and dissimilar type inside the interaction radius of i^{th} particle.

$P_{k=1,2}$ has value close to 1 if particles of k^{th} type are separated and is close to 0 if they are mixed. We observed that for $d \in (10, 15)$ two different types of particles form bands separated from each other on two sides of the interface and mainly moving along the $y-$ direction. We checked the system for two other choices of random noise: $\phi \in (-0.8\pi, +1.2\pi)$ and $\phi \in (-1.2\pi, +0.8\pi)$ for two types and find the same results. In fig.9 we show the plot of $P(d) = \langle P_{1,2} \rangle$ as a function of junction width d . $\langle \dots \rangle$, stands for average over two type of particles. $P(d)$ shows a peak for $d = 14$ and then decreases on increasing and decreasing d from it. Hence for intermediate values of interface width $d \simeq 14$, the two types of particles are maximally separated from each other. Remember this range of d where we find the maximum separation is the same where we find a transition to switching current.

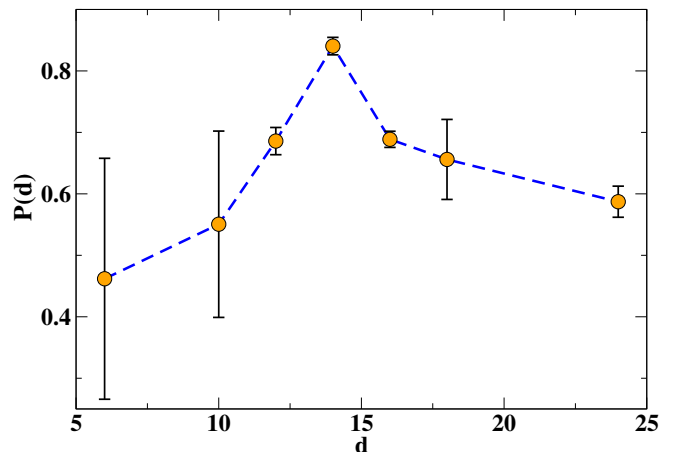


FIG. 9: (color online) Plot of phase separation order parameter $P(d)$ vs. interface width d . $L \times W = 200 \times 5, \rho = 1.0$

V. SUMMARY AND DISCUSSION

We have studied the properties of collection of polar self-propelled particles moving on a two dimensional rectangular channel along an order-disorder interface with periodic boundary condition in both directions. The interaction among the particles is taken as Vicsek type viz; particles move with constant speed and interact through short range alignment interaction. Inside the junction or disorder region, particles experience a high noise disorder state, and outside they are in the ordered state. The width of the junction is adjusted by the junction width d . The model is motivated by the Josephson junction, an analogous equilibrium system in solid state [49]. We studied the system for the two cases: (i) system WOP, where we do not impose any easy direction for moving SPPs and (ii) system WP where a small external biased direction of motion along the long axis of the channel is introduced. Interestingly, flock experience more dis-

turbance at wider junction width in the system WP in comparison to the system WOP. On increasing width of the junction, the system WOP shows a very small change in the global orientation of particles, whereas for the system WP, it shows transition from macroscopic ordered to disordered state. At the junction, we have found the current reversal for a range of intermediate widths of the junction. Such current reversal is due to the reflection of particles from the walls of the interface for intermediate junction widths.

Further, we also modeled a binary system of two-types of the particle in the system and find that the two type of particles show macroscopic phase separation for the same intermediate width of the interface. Hence such geometry can also be used for the sorting of different types of particles.

To the best of our knowledge this kind of study for SPPs at interface has not been explored yet. Although similar setups have been explored in experiments and theory for magnetic devices showing interesting properties [57, 58]. A detail comparison of our results obtained here with

these studies is our future work. We believe that the results presented here can be tested in experiments by designing such system. Our study also provide new scopes in active matter systems where particles experiences different environment along their move. The results presented here can be useful to understand the manufacturing of variety of practical devices using biological agents: mechanical circuits, switching devices, geophysical sensors, etc.

VI. ACKNOWLEDGEMENT

J.P, P.S.M, V.S. and S. M., thanks PARAM Shivay for computational facility under the National Supercomputing Mission, Government of India at the Indian Institute of Technology, Varanasi and the computational facility at I.I.T. (BHU) Varanasi. P.S.M. thanks UGC for research fellowship. V.S. thanks DST IN-SPIRE (INDIA) for the research fellowship. S.M. thanks DST, SERB (INDIA), Project No.: CRG/2021/006945, MTR/2021/000438 for financial support.

-
- [1] F. Ndlc, T. Surrey, A. C. Maggs, and S. Leibler, *Nature* **389**, 305 (1997).
 - [2] Y. Harada, A. Noguchi, A. Kishino, and T. Yanagida, *Nature* **326**, 805 (1987).
 - [3] M. Turkina and O. Sokolov, *Russian Journal of Plant Physiology* **48**, 681 (2001).
 - [4] S. J. Kron and J. A. Spudich, *Proceedings of the National Academy of Sciences* **83**, 6272 (1986).
 - [5] M. T. Laub and W. F. Loomis, *Molecular biology of the cell* **9**, 3521 (1998).
 - [6] S. Pattanayak, J. P. Singh, M. Kumar, and S. Mishra, *Physical Review E* **101**, 052602 (2020).
 - [7] T. Vicsek, A. Czirók, E. Ben-Jacob, I. Cohen, and O. Shochet, *Physical review letters* **75**, 1226 (1995).
 - [8] J. P. Singh, S. Pattanayak, and S. Mishra, *Journal of Physics A: Mathematical and Theoretical* **54**, 115001 (2021).
 - [9] P. K. Mishra and S. Mishra, *Physics of Fluids* **34**, 057110 (2022).
 - [10] J. Toner and Y. Tu, *Physical review letters* **75**, 4326 (1995).
 - [11] J. P. Singh and S. Mishra, *Physica A: Statistical Mechanics and its Applications* **544**, 123530 (2020).
 - [12] M. C. Marchetti, J.-F. Joanny, S. Ramaswamy, T. B. Liverpool, J. Prost, M. Rao, and R. A. Simha, *Reviews of modern physics* **85**, 1143 (2013).
 - [13] G. Grégoire and H. Chaté, *Physical review letters* **92**, 025702 (2004).
 - [14] H. Chaté, F. Ginelli, G. Grégoire, and F. Raynaud, *Physical Review E* **77**, 046113 (2008).
 - [15] B. Bhattacharjee, S. Mishra, and S. S. Manna, *Phys. Rev. E* **92**, 062134 (2015).
 - [16] V. Narayan, S. Ramaswamy, and N. Menon, *Science* **317**, 105 (2007).
 - [17] R. Bechinger, *Rev. Mod. Phys* **88**, 045006 (2016).
 - [18] L. Angelani, R. Di Leonardo, and G. Ruocco, *Physical review letters* **102**, 048104 (2009).
 - [19] J. Harder, S. Mallory, C. Tung, C. Valeriani, and A. Cacciuto, *The Journal of chemical physics* **141**, 194901 (2014).
 - [20] S. Pattanayak, J. P. Singh, M. Kumar, and S. Mishra, *Physical Review E* **101**, 052602 (2020).
 - [21] P. De Castro and P. Sollich, *Physical Chemistry Chemical Physics* **19**, 22509 (2017).
 - [22] V. Semwal, J. Prakash, and S. Mishra, *arXiv preprint arXiv:2112.13015* (2021).
 - [23] S. Pattanayak, R. Das, M. Kumar, and S. Mishra, *The European Physical Journal E* **42**, 1 (2019).
 - [24] V. Semwal, S. Dikshit, and S. Mishra, *The European Physical Journal E* **44**, 1 (2021).
 - [25] A. Baskaran and M. C. Marchetti, *Physical Review Letters* **101**, 268101 (2008).
 - [26] J. P. Singh, S. Pattanayak, S. Mishra, and J. Chakrabarti, *The Journal of Chemical Physics* **156**, 214112 (2022).
 - [27] I. Buttinoni, J. Bialké, F. Kümmel, H. Löwen, C. Bechinger, and T. Speck, *Physical review letters* **110**, 238301 (2013).
 - [28] M. E. Cates and J. Tailleur, *Annu. Rev. Condens. Matter Phys.* **6**, 219 (2015).
 - [29] E. Sese-Sansa, I. Pagonabarraga, and D. Levis, *Europhysics Letters* **124**, 30004 (2018).
 - [30] S. Dikshit and S. Mishra, *The European Physical Journal E* **45**, 21 (2022).
 - [31] S. Dikshit and S. Mishra, *The European Physical Journal E* **45**, 21 (2022).
 - [32] N. Chaffey, (2003).
 - [33] R. J. Hawkins, M. Piel, G. Faure-Andre, A. M. Lennon-Dumenil, J. F. Joanny, J. Prost, and R. Voituriez, *Phys. Rev. Lett.* **102**, 058103 (2009).

- [34] S. Das, A. Garg, A. I. Campbell, J. Howse, A. Sen, D. Velegol, R. Golestanian, and S. J. Ebbens, *Nature communications* **6**, 8999 (2015).
- [35] W. Uspal, M. N. Popescu, S. Dietrich, and M. Tasinkevych, *Soft matter* **11**, 434 (2015).
- [36] G. Volpe, I. Buttinoni, D. Vogt, H.-J. Kümmerer, and C. Bechinger, *Soft Matter* **7**, 8810 (2011).
- [37] A. Mozaffari, N. Sharifi-Mood, J. Koplik, and C. Maldarelli, *Physics of Fluids* **28**, 053107 (2016).
- [38] G. Saracco, G. Gonnella, D. Marenduzzo, and E. Orlandini, *Physical Review E* **84**, 031930 (2011).
- [39] S. Mishra and S. Pattanayak, *Physica A: Statistical Mechanics and its Applications* **477**, 128 (2017).
- [40] E. Bodenschatz, W. Pesch, and G. Ahlers, *Annual review of fluid mechanics* **32**, 709 (2000).
- [41] A. Zumdieck, R. Voituriez, J. Prost, and J. Joanny, *Faraday discussions* **139**, 369 (2008).
- [42] R. Voituriez, J. F. Joanny, and J. Prost, *EPL (Europhysics Letters)* **70**, 404 (2005), arXiv:q-bio/0503022 [q-bio.SC].
- [43] A. Zumdieck, R. Voituriez, J. Prost, and J. F. Joanny, *Faraday Discuss* **139**, 369 (2008).
- [44] X. Wang, M. In, C. Blanc, M. Nobili, and A. Stocco, *Soft Matter* **11**, 7376 (2015).
- [45] A. Dominguez, P. Malmaretti, M. Popescu, and S. Dietrich, *Soft matter* **12**, 8398 (2016).
- [46] P. Malmaretti, M. Popescu, and S. Dietrich, *Soft Matter* **12**, 4007 (2016).
- [47] K. Dietrich, D. Renggli, M. Zanini, G. Volpe, I. Buttinoni, and L. Isa, *New Journal of Physics* **19**, 065008 (2017).
- [48] T. Kontos, M. Aprili, J. Lesueur, F. Genêt, B. Stephanidis, and R. Boursier, *Physical review letters* **89**, 137007 (2002).
- [49] B. D. Josephson, *Physics letters* **1**, 251 (1962).
- [50] A. I. Buzdin, L. Bulaevskii, and S. Panyukov, *JETP lett* **35**, 178 (1982).
- [51] T. Kontos, M. Aprili, J. Lesueur, and X. Grison, *Physical review letters* **86**, 304 (2001).
- [52] I. Kulik, *Soviet Journal of Experimental and Theoretical Physics* **22**, 841 (1966).
- [53] J. P. Singh, S. Kumar, and S. Mishra, *Journal of Statistical Mechanics: Theory and Experiment* **2021**, 083217 (2021).
- [54] H. Chaté, F. Ginelli, G. Grégoire, and F. Raynaud, *Physical Review E* **77**, 046113 (2008).
- [55] S. Mishra, A. Baskaran, and M. C. Marchetti, *Physical Review E* **81**, 061916 (2010).
- [56] For our current system parameters with $\rho = 1.0$, $v_0 = 0.5$, $L \times W = 200 \times 5$, with no interface and $\eta = 0.3$: the typical width of band we found is $\simeq (10)$.
- [57] R. Gurzhi, A. Kalinenko, A. Kopeliovich, A. Yanovsky, E. Bogachek, and U. Landman, *Journal of superconductivity* **16**, 201 (2003).
- [58] G. Schmidt, G. Richter, P. Grabs, C. Gould, D. Ferrand, and L. Molenkamp, *Physical Review Letters* **87**, 227203 (2001).